

NuSTAR observation of Ark 564 reveals the variation of coronal temperature with flux

Samuzal Barua^{1*}, V. Jithesh^{2†}, Ranjeev Misra^{2‡}, Gulab C Dewangan²,
Rathin Sarma³ and Amit Pathak⁴

¹*Department of Physics, Gauhati University, Jalukbari, Guwahati-781014, Assam, India*

²*Inter-University Centre for Astronomy and Astrophysics (IUCAA), PB No.4, Ganeshkhind, Pune-411007, India*

³*Department of Physics, Rabindranath Tagore University, Hojai-782435, Assam, India*

⁴*Department of Physics, Banaras Hindu University, Varanasi-221005, India*

Accepted XXX. Received YYY; in original form ZZZ

ABSTRACT

The hard X-ray spectral index of some AGN has been observed to steepen with the source flux. This has been interpreted in a Comptonization scenario, where an increase in the soft flux decreases the temperature of the corona, leading to steepening of the photon index. However, the variation of the coronal temperature with flux has been difficult to measure due to the presence of complex reflection component in the hard X-rays and the lack of high-quality data at that energy band. Recently, a 200 ks *NuSTAR* observation of Ark 564 in 3–50 keV band, revealed the presence of one of the coolest coronae with temperature $kT_e \sim 15$ keV in the time-averaged spectrum. Here, we re-analyse the data and examined the spectra in four flux levels. Our analysis shows that the coronal temperature decreased from ~ 17 to ~ 14 keV as the flux increased. The high energy photon index $\Gamma \sim 2.3$ varied by less than 0.1, implying that the optical depth of the corona increased by about 10% as the flux increased. This first reporting of coronal temperature variation with flux shows that further long observation by *NuSTAR* of this and other sources would shed light on the geometry and dynamics of the inner regions of the accretion flow.

Key words: black hole physics – galaxies: active – galaxies: Seyfert – X-rays: individual: Ark 564

1 INTRODUCTION

An important characteristic Narrow-line Seyfert 1 (NLS1) galaxies is that they typically show extreme variability in the X-ray band (Remillard et al. 1991; Boller et al. 1997; Brandt & Boller 1998; Brandt et al. 1999). It is believed that they harbour smaller black holes and accrete at near Eddington limit (Pounds et al. 1995; Collin & Kawaguchi 2004) compared to standard Active Galactic Nuclei (AGN). NLS1s generally show strong soft X-ray excess below 2 keV, and their spectral slopes are somewhat steeper (Boller et al. 1996; Brandt et al. 1997; Turner et al. 1998; Leighly 1999b; Vaughan et al. 1999a).

It is nearly a standard paradigm, that the X-ray power law emission of AGN, is due to inverse-Compton scattering of soft photons from a standard accretion disc, by the elec-

trons of an hot corona (Sunyaev & Truemper 1979). The Comptonized spectra from the hot thermal corona impinge on the standard disk resulting in a reflected component detected by a fluorescent iron line peaking at ~ 6.4 keV and a Compton reflection hump at 20–100 keV (George & Fabian 1991). One can fit broadband X-ray data with a thermal Comptonization model and corresponding reflection component to obtain an estimate of the coronal temperature. However, till recently, it was difficult to do so because of the low sensitivity of detectors in this energy range and the complexities arising from modelling the reflection component.

The Nuclear Spectroscopic Telescope Array (*NuSTAR*) is the first hard X-ray focusing telescope in orbit (Harrison et al. 2013), which operates in the 3–79 keV X-ray band, extending the sensitivity of focusing optics far beyond the ~ 10 keV high-energy cutoff achieved by all previous X-ray satellites. García et al. (2015) have shown that with these specifications, it is possible to measure the temperature (or the high energy cutoff) of AGN coronae from spectral analysis of *NuSTAR* data. Indeed a long observation of Ark 564 by

* E-mail: samuzal.barua@gmail.com

† E-mail: vjithesh@iucaa.in

‡ E-mail: rmisra@iucaa.in

NuSTAR revealed the presence of a low temperature corona ($kT_e \sim 15$ keV; Kara et al. 2017, hereafter EK17). Recently, *NuSTAR* observations provided estimates of low temperatures ($kT_e \sim 20$ keV) of the corona for two more AGN (Buisson et al. 2018).

As mentioned earlier, AGN in general, and NLS1s, in particular, are highly variable in both flux and spectral shape and the correlation between them, provide insight into their nature. One of the interesting variable property, they share with X-ray binaries is that typically the high energy photon index correlates positively with the low energy flux (for e.g. Haardt et al. 1997; Zdziarski et al. 2003; Sobolewska & Papadakis 2009; Sarma et al. 2015). In other words, the high energy spectrum steepens with increasing soft flux. It has been argued that this may be a natural consequence of the Comptonization (Zdziarski et al. 2003). If the flux of the input seed photons (i.e. the soft photons) increases, the radiative cooling of the corona increases. Since the radiative cooling efficiency is very high there must be heating of the corona to maintain a high temperature (Fabian et al. 2015). If this heating rate does not vary (or if it does not increase in the same proportion as the input flux) this would lead to a decrease in the temperature of the corona. This in turn would cause high energy spectra to steepen as observed. Although this interpretation is attractive and seems natural, it should be noted that up till now there has been no direct evidence for the coronal temperature to decrease with flux. There are indirect ways to infer that the temperature decreases with flux. For example for Mrk 335, Wilkins & Gallo (2015) measured the expansion of the corona with flux, which when combined with the change in photon index, implied that the coronal temperature must have decreased.

The long (~ 200 ks) *NuSTAR* observation of Ark 564, where the coronal temperature was found to be ~ 15 keV (EK17) in the time averaged spectrum, provides a unique opportunity to test the hypothesis of the coronal temperature varying with flux. Ark 564 is a X-ray bright NLS1 galaxy at a red-shift $z = 0.02469$ (Huchra et al. 1999) with a 2–10 keV flux of $\sim 2 \times 10^{-11}$ erg cm $^{-2}$ s $^{-1}$ (Vaughan et al. 1999b) and the corresponding luminosity is $\sim 2.4 \times 10^{43}$ erg s $^{-1}$ (Turner et al. 2001). The source shows rapid variability, a very steep spectrum in the 0.3–10 keV band, strong soft excess and iron K emission line (Turner et al. 1999; Leighly 1999a; Turner et al. 2001). Analysis of a number of *XMM-Newton* observations suggest that this high-Eddington NLS1 exhibits a prominent correlation between spectral slope and flux (Sarma et al. 2015). EK17 report that during the *NuSTAR* observation, the source exhibited a dramatic flare, in which the hard emission is delayed with respect to the soft one. Indeed the flux of the source varied by about a factor of two, and hence it should be possible to verify whether the coronal temperature also varied.

Here, we re-analyse the 200 ks *NuSTAR* observation to investigate whether any correlation or trend exists between the coronal electron temperature and flux of the X-ray luminous source Ark 564. The paper is organized as follows: In §2, we describe the observations and analysis. In §3, we present the results of the spectral fitting analyses of time-averaged as well as the flux resolved spectra and discuss the interpretations of these results in §4.

2 OBSERVATION AND DATA ANALYSIS

Ark 564 was observed with *NuSTAR* on 2015 May 22 for an exposure time of ~ 200 ks. The *NuSTAR* data were reduced and cleaned for high background flare with the NUPIPELINE script using *NuSTAR* data analysis software (NUSTARDAS) v1.8.0 and CALDB version 20171002 to obtain calibrated event files in Level 1 data products. We used a circular source region of 50 arcsec radius and a slightly larger background region of 60 arcsec for both the detectors, Focal Plane Modules A and B (FPMA and FPMB). With NUPRODUCTS task, we extracted FPMA/FPMB spectra and light curves together with the redistribution matrix files (RMF) and ancillary response files (ARF). We grouped FPMA and FPMB time-averaged spectra using GRPPHA tool with 50 counts in each spectral bin. Additionally as advised by García et al. (2015), we binned the source spectra, background spectra and RMF in order to acquire the proper sampling of the data, which originally had equal bin width of 0.04 keV throughout the entire X-ray band. In particular, we used a binning of 0.16 keV for data below 20 keV and a binning of 0.32 keV in the 20–50 keV band.

3 SPECTRAL RESULTS

3.1 Time-averaged spectrum

We first reproduce the spectral results obtained by EK17. For that, we fitted the time-averaged spectrum from both FPMA and FPMB detectors simultaneously in the 3–50 keV energy band using the ionized reflection model *xillverCp*¹, where the continuum is modelled as being due to Comptonization (i.e. the XSPEC (Arnaud 1996) model *nthComp*; Zdziarski et al. 1996; Życki et al. 1999) and the corresponding ionized reflection. We allowed for the possibility that relative normalization between the two instruments may vary, by including a constant to the model for the FPMB spectrum. Errors on best-fit parameters were obtained from the Markov chain Monte Carlo (MCMC) analysis by using the XSPEC-EMCEE code². We use the Goodman-Weare algorithm by specifying 60 walkers with 12,000 iterations to calculate the best-fit parameters and their uncertainty (see more details in EK17). The best-fit parameters with errors from our analysis of the time-averaged spectrum are listed in Table 1. The best-fit parameter values correspond to the peaks of the marginalized probability distribution. The quoted parameter errors are at a 90% confidence level. The reported spectral parameters in EK17 such as electron temperature, $kT_e = 15_{-1}^{+2}$ keV, the photon index $\Gamma = 2.32_{-0.01}^{+0.02}$, reflection fraction $R = 1.18_{-1.18}^{+2.10}$ and disc ionization parameter, $\log \xi = 4.43 \pm 0.06$ are consistent with our analysis, but other parameters are marginally different from our results. The minor deviation in the parameters may be due to the use of older versions of *xillverCp* model, *NuSTAR* software package (version 1.6.0) and CALDB (version 20160502) in EK17 as compared to this analysis.

Having obtained the spectral parameters similar to

¹ <http://www.sternwarte.uni-erlangen.de/~dauser/research/relxill/>

² https://github.com/jeremysanders/xspec_emcee

Table 1. Spectral parameters from the simultaneous fits of *NuSTAR* FPMA and FPMB time-averaged spectra in 3–50 keV band using model *xillverCp*. From left to right the model parameters are photon index (Γ), iron abundance (Afe), temperature of corona electrons (kT_e), log of the ionization parameter or accretion disk ionization (ξ), inclination of the accretion disk (θ), reflection fraction (R), normalization, flux ($F_{3-50\text{ keV}}$) and reduced χ^2 with degrees of freedom respectively.

Γ	Afe solar	kT _e keV	log ξ log(erg cm s ⁻¹)	θ degree	R	Norm 10 ⁻⁴	$F_{3-50\text{ keV}}$ 10 ⁻¹¹ erg cm ⁻² s ⁻¹	χ^2_r /d.o.f
$2.30^{+0.040}_{-0.001}$	$2.24^{+0.10}_{-0.45}$	$14.97^{+1.89}_{-0.79}$	$4.65^{+0.01}_{-0.23}$	$30.97^{+7.06}_{-3.76}$	$1.23^{+1.30}_{-0.65}$	$0.45^{+0.36}_{-0.19}$	$1.93^{+0.01}_{-0.01}$	1.02/619

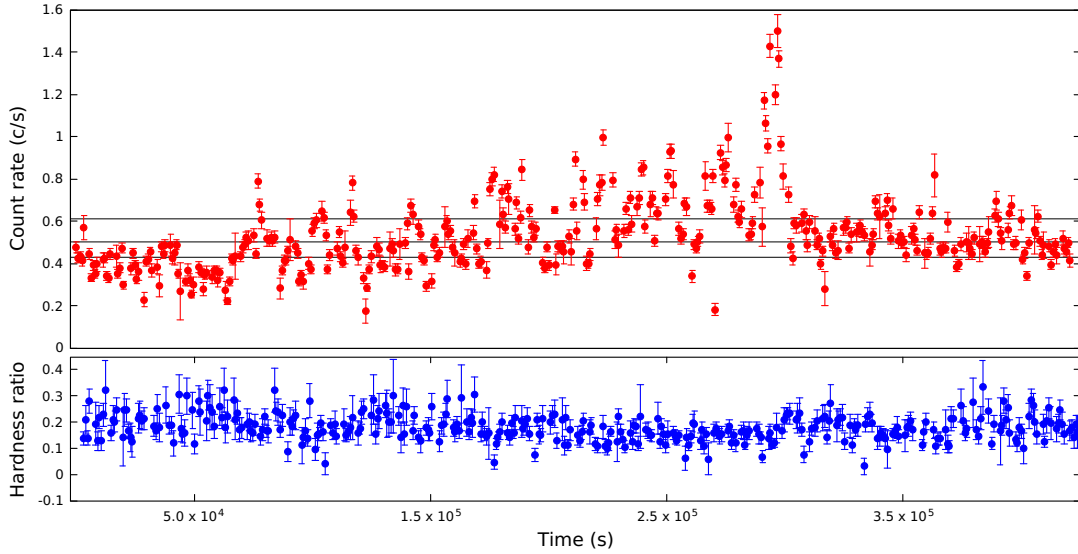


Figure 1. The light curve of Ark 564 from the *NuSTAR* observation with a total exposure time of 200 ks. The light curve is produced with a time bin size of 800 s. The black horizontal lines divide the light curve into four flux levels. The hardness ratio, depicted in the bottom panel, derived from the 3–10 keV and 10–50 keV energy bands.

those obtained by EK17, we proceed to do flux resolved spectroscopy to investigate if the coronal temperature shows any variation with flux.

3.2 Flux-resolved spectroscopy

To extract the spectra for different flux states, the FPMA and FPMB light curves were generated with a time bin of 800 s in the complete energy range of 3–79 keV. The two light curves were then added and the resultant variation of count rate with time is shown in Figure 1. A flare has been detected during the observation of Ark 564, which is shown in the light curve. The 3–79 keV mean count rates of the source in FPMA and FPMB are 0.28 c/s and 0.27 c/s, respectively. In order to investigate the flux resolved spectra of Ark 564, the light curve is split into four flux levels. The light curve is divided in such a way that each level contains an approximately equal number of bins, i.e., roughly 25 percent of the total number of bins. The four levels are designated as very low (< 0.42 c/s), low (between 0.42 and 0.5 c/s), high (between 0.5 and 0.61 c/s) and very high (> 0.61 c/s) are shown in Figure 1. The source spectra for both FPMA and FPMB along with the associated files are extracted in a similar way as explained for the time-averaged spectra.

To quantify the spectral shape difference between the four flux states in a model-independent way, we fit the spectra in the energy range 3–5 keV, with a power-law and then

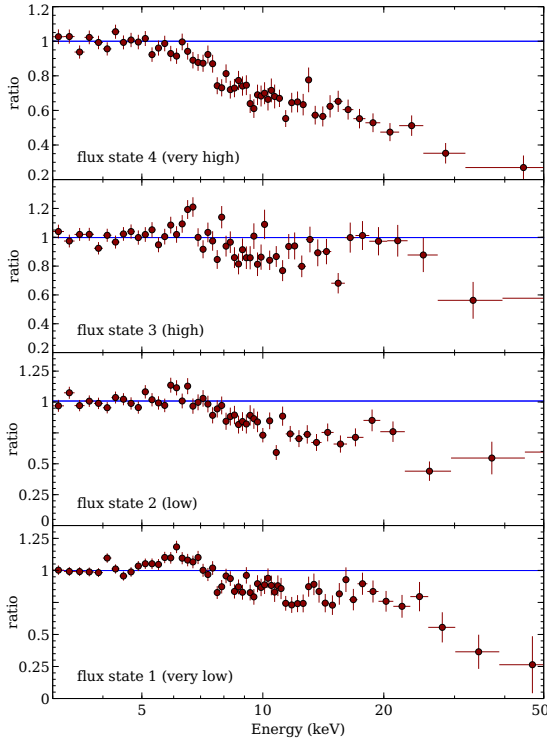
show the ratio of the data to the model for the full 3–50 keV range in Figure 2. While high energy curvature is seen in all states, it is largest for the highest flux state, indicating perhaps that the coronal temperature is lowest at that state.

We then use the four flux levels to study the detailed flux resolved spectroscopy of the source. We use the data in the 3–50 keV energy band and fitted FPMA and FPMB spectra simultaneously with the same reflection model *xillverCp*. The flux resolved spectra from the four levels are shown in Figure 3. We fix the iron abundance (Afe) and inclination (θ) to the values obtained from the time-averaged spectrum and kept the other parameters free. This model described the observed spectra in different flux levels and we obtained a satisfactory fit in all cases. We estimated the flux in the energy range 3–50 keV using the XSPEC model *cflux*. It is seen from the flux resolved spectral fitting that the flux of Ark 564 changed abruptly in the fourth state (highest flux state) as compared to the other three states. The best-fit spectral parameters with errors are tabulated in Table 2 and the variation of the temperature and index with flux are shown in Figure 4. We detect a temperature drop from ~ 17 keV to ~ 14 keV when the flux increases.

To test the significance of the variation of the temperature with flux, we fitted a constant to the four data points. This resulted in a χ^2 of 8.5 for 3 degrees of freedom, which translates to a null hypothesis probability of 1.2×10^{-5} that the temperature did not vary with flux. The fitting degen-

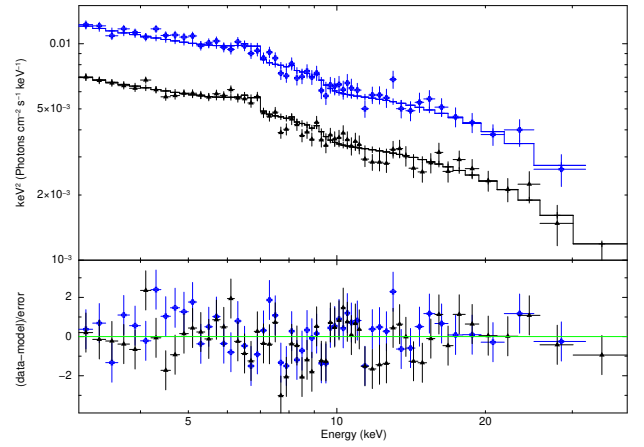
Table 2. Spectral Parameters from the flux resolved spectroscopy of Ark 564 for the four flux levels. In all spectral fits, the inclination (θ) and iron abundance (Afe) parameters are fixed at the values obtained from the time-averaged spectral fit.

Flux State	Γ	kT_e keV	$\log\xi$ $\log(\text{erg cm s}^{-1})$	R	Norm 10^{-4}	$F_{3-50 \text{ keV}}$ $10^{-11} \text{ erg cm}^{-2} \text{ s}^{-1}$	χ_r^2 /d.o.f
1	$2.31^{+0.04}_{-0.05}$	$17.41^{+0.92}_{-0.67}$	$4.44^{+0.14}_{-0.16}$	$1.22^{+1.27}_{-1.17}$	$0.37^{+0.02}_{-0.01}$	$1.62^{+0.01}_{-0.01}$	1.11/416
2	$2.32^{+0.04}_{-0.04}$	$17.09^{+0.91}_{-0.77}$	$4.32^{+0.21}_{-0.12}$	$1.10^{+1.14}_{-1.05}$	$0.47^{+0.02}_{-0.02}$	$1.78^{+0.01}_{-0.01}$	1.06/316
3	$2.32^{+0.05}_{-0.05}$	$16.04^{+0.77}_{-0.80}$	$4.60^{+0.21}_{-0.24}$	$1.12^{+1.18}_{-1.07}$	$0.49^{+0.03}_{-0.02}$	$1.95^{+0.01}_{-0.01}$	1.18/331
4	$2.35^{+0.08}_{-0.08}$	$14.01^{+0.56}_{-1.06}$	$4.69^{+0.30}_{-0.27}$	$1.12^{+1.19}_{-1.06}$	$0.79^{+0.04}_{-0.05}$	$2.82^{+0.02}_{-0.02}$	1.01/365

**Figure 2.** Data-model ratio from the power law fits of four *NuSTAR* FPMA flux resolved spectra. All of the FPMA spectra are grouped, and a standard binning is applied using XSPEC.

eracy between the spectral parameters and their distributions are shown for the very low and very high flux states in Figure 5. While the temperature is moderately degenerate with $\log \xi$ and Γ , it should be noted that with flux it is only marginally correlated and that to positively. Thus the observed anti-correlation between the temperature and flux should not be affected by this fitting degeneracy.

The coronal temperature is statistically consistent between the lowest three flux bins, while significant variation is only seen in the highest bin. We attempted to get a better constraint by binning the first three flux points into one and fitting the average spectrum. The best fit temperature turned out to be $17.05^{+0.9}_{-0.5}$ keV, and the error bars did not

**Figure 3.** The *NuSTAR* FPMA spectra from the lowest (black triangle) and highest (blue plus) flux states fitted with xillverCp. All 3–50 keV spectra are grouped and binned as mentioned in §2.

significantly decrease compared to those obtained for the three individual flux bins.

4 DISCUSSION

The flux resolved spectroscopy of Ark 564 undertaken in this work, indicates that the coronal temperature decreases as the flux increases. For the modelling, the reflection fraction and the ionization parameter are allowed to vary but are not well constrained. We note that the coronal temperature variation is detected even when these parameters are allowed to vary.

As shown in the middle panel of Figure 4, the photon index Γ does not vary with flux significantly. The variation in Γ is less than 0.1, even though the flux varied roughly by a factor of two. For Comptonization emission, the optical depth τ is related to the temperature kT_e and photon index by (Zdziarski et al. 1996; Zycki et al. 1999),

$$\tau = \sqrt{\frac{9}{4} + \frac{3}{\theta \left[\left(\Gamma + \frac{1}{2} \right)^2 - \frac{9}{4} \right]}} - \frac{3}{2} \quad (1)$$

where $\theta = kT_e/m_e c^2$. The bottom panel of Figure 4

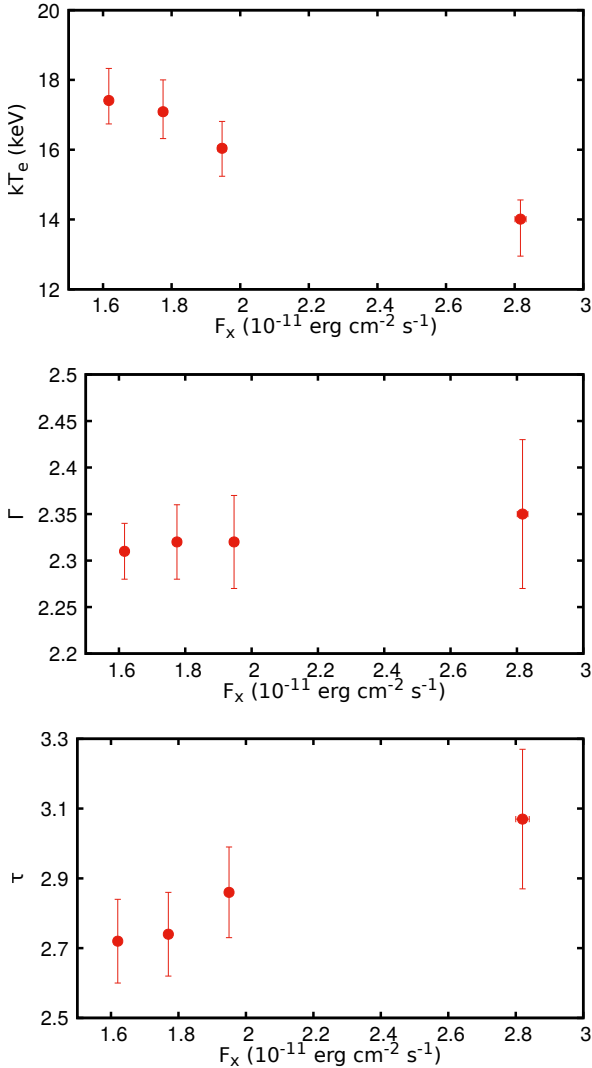


Figure 4. The variation of coronal electron temperature (*top* panel), the photon index (*middle* panel) and the optical depth (*bottom* panel) with the 3–50 keV flux.

shows the variation of τ with flux as inferred from the above equation. Thus, a 10% increase in the optical depth (from $\tau \sim 2.7$ to $\tau \sim 3.1$) may explain why the photon index did not vary between the low and hard flux states despite the variation in temperature. If the optical depth has remained constant at ~ 2.7 , the photon index would have increased to ~ 2.6 from ~ 2.3 and may have been measurable. Thus, it is possible that if the optical depth varies, then the correlation between the flux and the photon index may not that strong. In addition, the variation in the optical depth suggests intrinsic variations in the corona rather than just cooling of corona by seed UV photons.

Like several other AGN, Ark 564 is known to have complex warm absorbers (Dewangan et al. 2007; Papadakis et al. 2007; Giustini et al. 2015), but since the energy band being considered here is 3–50 keV, these features may not affect the overall result presented here. While the *NuSTAR* data analysed does not require a relativistically smeared reflection component, such a complex component may affect

the estimation of the coronal temperature. Apart from these caveats, the measurement of coronal temperature at different flux levels of such sources from long *NuSTAR* observations, will be an important step towards understanding the nature and geometry of the inner regions of the accretion disks.

In summary, we show using flux resolved spectroscopy of *NuSTAR* observation of Ark 564, evidence that the coronal temperature decreases with flux. While, the inverse correlation between the coronal temperature and flux has been inferred indirectly using observed relations between spectral index and flux, this is the first direct evidence for such a behaviour. We further infer that the optical depth of the corona changes with flux, revealing a complex temporal behaviour of the inner regions of the accretion flow.

ACKNOWLEDGEMENTS

We thank the anonymous referee for the constructive comments and suggestions that improved this manuscript. SB acknowledges IUCAA Visitors programme and thank Jermy Sanders for the detailed discussion on the `XSPEC-EMCEE` code. RS and AP acknowledge the visiting associateship programme of IUCAA. SB, RS, AP & RM acknowledge the SERB research grant EMR/2016/005835. This research has made use of data obtained from the High Energy Astrophysics Science Archive Research Center (HEASARC), provided by NASA’s Goddard Space Flight Center, and the *NuSTAR* Data Analysis Software (NUSTARDAS) jointly developed by the ASI Science Data Center (ASDC, Italy) and the California Institute of Technology (Caltech, USA).

REFERENCES

- Arnaud K. A., 1996, in Jacoby G. H., Barnes J., eds, *Astronomical Society of the Pacific Conference Series Vol. 101, Astronomical Data Analysis Software and Systems V*. p. 17
- Boller T., Brandt W. N., Fink H., 1996, *A&A*, **305**, 53
- Boller T., Brandt W. N., Fabian A. C., Fink H. H., 1997, *MNRAS*, **289**, 393
- Brandt N., Boller T., 1998, *Astronomische Nachrichten*, **319**, 163
- Brandt W. N., Mathur S., Elvis M., 1997, *MNRAS*, **285**, L25
- Brandt W. N., Boller T., Fabian A. C., Ruszkowski M., 1999, *MNRAS*, **303**, L53
- Buisson D. J. K., Fabian A. C., Lohfink A. M., 2018, *Monthly Notices of the Royal Astronomical Society*, 481, 4419
- Collin S., Kawaguchi T., 2004, *A&A*, **426**, 797
- Dewangan G. C., Griffiths R. E., Dasgupta S., Rao A. R., 2007, *ApJ*, **671**, 1284
- Fabian A. C., Lohfink A., Kara E., Parker M. L., Vasudevan R., Reynolds C. S., 2015, *MNRAS*, **451**, 4375
- García J. A., Dauser T., Steiner J. F., McClintock J. E., Keck M. L., Wilms J., 2015, *ApJ*, **808**, L37
- George I. M., Fabian A. C., 1991, *MNRAS*, **249**, 352
- Giustini M., Turner T. J., Reeves J. N., Miller L., Legg E., Kraemer S. B., George I. M., 2015, *A&A*, **577**, A8
- Haardt F., Maraschi L., Ghisellini G., 1997, *ApJ*, **476**, 620
- Harrison F. A., et al., 2013, *ApJ*, **770**, 103
- Huchra J. P., Vogeley M. S., Geller M. J., 1999, *ApJS*, **121**, 287
- Kara E., García J. A., Lohfink A., Fabian A. C., Reynolds C. S., Tombesi F., Wilkins D. R., 2017, *MNRAS*, **468**, 3489
- Leighly K. M., 1999a, *ApJS*, **125**, 297
- Leighly K. M., 1999b, *ApJS*, **125**, 317

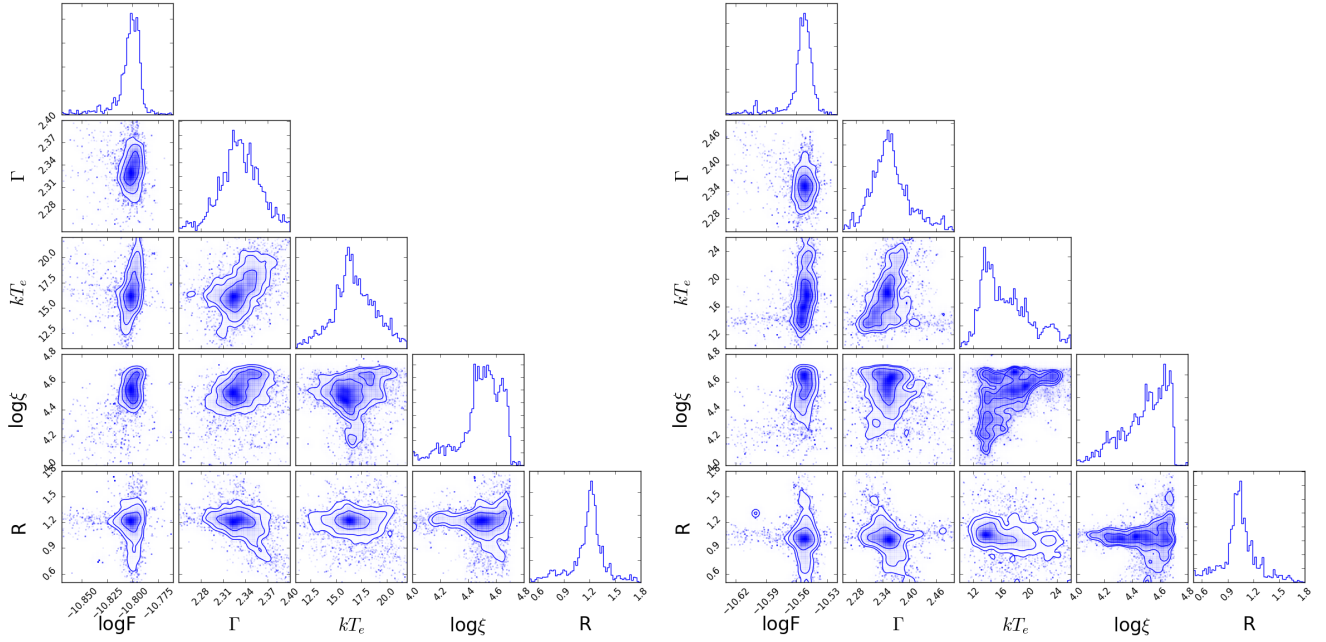


Figure 5. Corner plots of spectral parameters from MCMC analysis for the very low (left) and very high flux (right) states using `xillverCp` model. The one dimensional histograms represent the probability distribution, normalized to provide an area under the curve is equal to one. The units of $\log \xi$ and 3–50 keV flux are erg cm s^{-1} and $\text{erg cm}^{-2} \text{s}^{-1}$, respectively.

- Papadakis I. E., Brinkmann W., Page M. J., McHardy I., Uttley P., 2007, *A&A*, **461**, 931
- Pounds K. A., Done C., Osborne J. P., 1995, *MNRAS*, **277**, L5
- Remillard R. A., Grossan B., Bradt H. V., Ohashi T., Hayashida K., 1991, *Nature*, **350**, 589
- Sarma R., Tripathi S., Misra R., Dewangan G., Pathak A., Sarma J. K., 2015, *MNRAS*, **448**, 1541
- Sobolewska M. A., Papadakis I. E., 2009, *MNRAS*, **399**, 1597
- Sunyaev R. A., Truemper J., 1979, *Nature*, **279**, 506
- Turner T. J., George I. M., Nandra K., 1998, *ApJ*, **508**, 648
- Turner T. J., George I. M., Netzer H., 1999, *ApJ*, **526**, 52
- Turner T. J., Romano P., George I. M., Edelson R., Collier S. J., Mathur S., Peterson B. M., 2001, *ApJ*, **561**, 131
- Vaughan S., Reeves J., Warwick R., Edelson R., 1999a, *MNRAS*, **309**, 113
- Vaughan S., Reeves J., Warwick R., Edelson R., 1999b, *MNRAS*, **309**, 113
- Wilkins D. R., Gallo L. C., 2015, *MNRAS*, **449**, 129
- Zdziarski A. A., Johnson W. N., Magdziarz P., 1996, *MNRAS*, **283**, 193
- Zdziarski A. A., Lubiński P., Gilfanov M., Revnivtsev M., 2003, *MNRAS*, **342**, 355
- Życki P. T., Done C., Smith D. A., 1999, *MNRAS*, **309**, 561

This paper has been typeset from a $\text{\TeX}/\text{\LaTeX}$ file prepared by the author.